EVALUATION OF EPOXY RESINS FOR UNDER-THE-HOOD APPLICATIONS

Anthony M. Coppola, Ph.D.
General Motors

Abstract

In the past few decades, polymer-based materials have seen increasing usage as lightweight and low-cost alternatives to metals in many under-the-hood applications, such as reservoirs, component housings, engine intake manifolds, washers, gaskets, and more. However, concerns regarding their elevated temperature capability have limited their use to primarily non-structural applications. Significant lightweighting is achievable through mixed material designs utilizing polymer matrix composite materials. This work examines the structural capability of composites containing various epoxies as the matrix material at elevated temperatures relevant to under-the-hood use; i.e. from 23-220° C. Five different resin systems are evaluated under various mechanical tests and after various environmental exposure conditions. Monotonic tests include three-point flexure, short beam shear, tension, and compression. Dynamic mechanical analysis (DMA) is also conducted for each resin, and glass transition temperature results are linked to results from monotonic testing. The correlation between the glass transition temperature of the epoxy matrix and mechanical performance at elevated temperature of a composite formed from that epoxy is studied. The effect of long-term aging in air, oil, and engine coolant on mechanical performance of the epoxy-based composites is also evaluated.

Introduction

Under-the-hood applications in internal combustion engine powered vehicles pose some of the largest challenges to using polymer matrix composites (PMCs) in automotive applications due to the elevated temperatures present. Temperatures in an engine, for example, range from approximately 100-200°C but may reach several hundred degrees near the combustion chamber and exhaust ports [1,2]. PMCs may suffer reduced structural performance, cracking, excessive creep, mass loss, and even thermal degradation at elevated temperatures [3,4]. However, using PMCs in under-the-hood applications also presents a large opportunity. The engine block, for example, is among the heaviest single components in a vehicle, weighing from 20 to over 50 kg. The block also plays critical roles in transmission of engine noise and vibration to the passenger and in heat-up time for the engine. These roles make the engine block and other under-the-hood components high-value applications for PMCs. Primary concerns for PMCs under-the-hood include direct loss of properties with increasing temperature, thermo-oxidation, and moisture or other solvent absorption.

The most immediate effect of elevated temperature of PMCs is a loss in structural performance. Properties that are affected include tensile and compressive properties, fracture resistance, shear properties, impact resistance, and viscoelastic damping [5–9]. The service temperature for a PMC is generally set based on the glass transition temperature (T_g). Polymers transition from a glassy state below T_g to a rubbery state above T_g. This transition is characterized by significant reductions in stiffness and strength of the polymer above T_g, in addition to changes in the thermal expansion rate and heat capacity [10]. In the case of thermoset polymers, the reduction in stiffness and strength can be several orders of magnitude. However, these changes in material properties are reversible upon cooling of the composite below T_g, though permanent deformation of the component may occur. A general rule of thumb in the aerospace industry is to select a material with a T_g of 50°C above the use temperature. However, material cost generally

increases with increased T_g, making this impractical for many automotive applications.

Numerous options exist when selecting a matrix material for a composite. Common examples for thermoset resins, in rough order of increasing temperature resistance, include polyesters, polyurethanes, vinyl esters, epoxies, phenolics, benzoxazines, cyanate esters, bismaleimides, and polyimides [11,12]. The cost of the resin generally increases with increased temperature resistance, both between various polymer classes and within a single polymer class. Epoxies were selected as the focus of this study because they were found to have the best balance between cost and performance as a continuous-fiber-reinforced composite matrix. Resins considered in this study had a T_g ranging from approximately 140-220°C and were processable by liquid molding processes (*e.g.* resin transfer molding).

Investigation of matrix materials for under-the-hood applications requires a method for screening materials. Many standardized mechanical test methods exist for composites, yet little information is given in each regarding their sensitivity to temperature. Standards such as ASTM D3045, “Standard Practice for Heat Aging of Plastics Without Load” dictate the aging conditions but leave the mechanical test method to the user. Here, four of the most common mechanical tests, including flexure, short beam shear, compression, and tension, were compared as to their sensitivity to temperature and general ease of use. DMA results are linked to the monotonic test results, primarily through the measurement of T_g. The goal is to aid the selection of test methods for rapid screening of such materials when no specific loading scenario dictates the method.

In the long term, the effect of elevated temperature on the PMC is highly dependent on the media of exposure. Three common media of exposure for engine components were selected for evaluation, including hot air, engine oil, and engine coolant. The primary concern of hot air exposure is thermo-oxidation, while oil and coolant are more of a concern in regard to media absorption and chemical attack of the molecular chains. In both cases, thermal degradation will occur at sufficiently high temperatures and long exposure times as the polymer chains break down, though short exposures may actually improve thermal performance due to a post-curing effect. The general effects of each of these media has been well studied in the literature [13–17].

Thermo-oxidation leads to mass change, embrittlement, color change, and volumetric changes leading to cracking. Oxidation is a chemical change in the material and is irreversible, though may occur simultaneously with reversible processes, such changes associated with excursions above T_g [14]. Oxidation of materials occurs through diffusion from the oxygen-containing environment to the interior of the material and is non-uniform through the material thickness [18]. In fact, a sharp oxidized boundary layer is common because oxygen consumption through chemical reaction is faster than the diffusion [15]. The oxidized material often presents as a darkened layer near the surface of the material, which grows thicker as the oxidation progresses as a function of time and temperature. Oxidation may be unnoticeable on the interior of the material even while the surface is heavily altered. In applications where the PMC must be subjected to high temperature oxygen-containing environments, care must be taken in material selection. Thermo-oxidation resistance of a polymer is largely a function of its chemical composition and molecular structure [12]. Polymers with higher T_g, such has polyimides, often have better oxidation resistance than lower T_g materials like epoxy. However, the underlying origins of thermo-oxidation resistance and T_g differ; therefore, T_g does not entirely capture the oxidation resistance of a polymer, particularly within the same class of materials (*e.g.* epoxies). Thermo-oxidative resistance generally relates to the stability of the bonds, while glass transition temperature arises from molecular chain mobility [10]. Modeling of the thermo-oxidative response of a polymer is well studied and validated models exist for many materials [3,4,15].

Moisture absorption, unlike thermo-oxidation, is generally a reversible process; the exceptions

being chemistries that are vulnerable to hydrolysis or hysteresis. Epoxy chemistries based on DGEBA and amine-curing agents generally do not experience hydrolysis, while anhydride-cured DGEBA-based resins may in some cases [19]. Hysteresis in the moisture content is a result of bound water molecules that are difficult to remove even upon heating [20]. Moisture absorption leads to plasticization of the resin, reducing T_g [21]. For example, the T_g of Cytec CYCOM 977-20 epoxy resin is reduced from 199° C under dry conditions to 154° C after 1.1% moisture uptake in a 70° C, 85% humidity environment [22]. While the effect of moisture on epoxy is moderate compared to materials such as polyamides, it is still of concern when designing a structural component operating near the T_g. The plasticization effect of moisture absorption generally has little effect on the glassy state properties and therefore room temperature (*ca.* 20° C) properties are unaffected [14]. However, the reduction in T_g may greatly affect the elevated temperature performance, particularly near T_g. Epoxy-based matrix resins are generally considered resistant to oil and little literature is available studying this [14,17]. However, the concern of thermal degradation is still present.

Experimental Materials and Methods

Composite Specimen Manufacture

Composite panels were composed of triaxial braided fabric (QISO-H by A&P Technology) and epoxy resin. The fabric contained 12k and 24k T700 carbon fiber tows arranged in the 0° (axial), +60° (bias), and -60° (bias) directions to create a nominally quasi-isotropic fabric (Figure 1). Two epoxy resins were considered as listed in Table 1.

Composite panels were manufactured using pressure-pot molding in a closed rectangular mold. The mold had a single inlet and single outlet centered on opposing sides of a 444.5 x 444.5 mm cavity measuring 2.4 mm in depth. During molding, 5 layers of triaxial braided fabric were placed in the cavity, the cavity was closed, and vacuum was applied. Resin pre-heated to 50° C, then was injected into the part under 40 psi of air pressure in a pressure-pot. Once resin reached the outlet, the outlet was closed. However, resin injection was continued for up to 5 minutes to ensure full filling of the mold. Then, the inlet was closed and the part cured for the prescribed time. Note that the cure timer was started at the beginning of the injection, as opposed to at the time the inlet was closed. Once the parts were cured, they were removed from the mold and cooled to room temperature. They were then post-cured in a convection oven. Finished panels were machined to the desired coupon size using water-jet cutting.

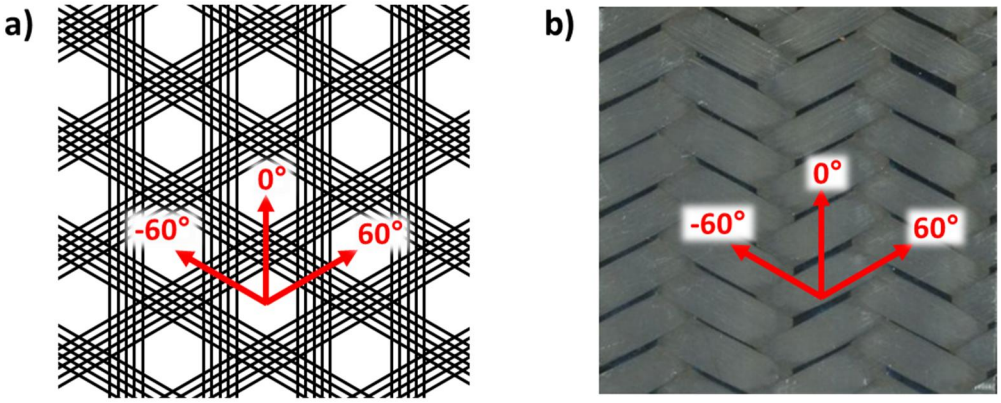

Figure 1: (a) Schematic and (b) composite photograph showing the structure of the triaxial braided fabric.

Table 1: Resins evaluated in this study and the cure/post-cure conditions for each.

	Resin	Hardener	Resin: Hardener Ratio, by mass	Cure Condition	Post-Cure Condition
D383/BV-ME-PS2	DOW DER 383 (epoxy)	Broadview Chemical BV-ME-PS2 (rubber toughened anhydride)	100:88	20 min @ 130° C	60 min @ 170° C
H3598/2954	Huntsman Araldite 3598 (nano-toughened epoxy)	Huntsman Aradur 2954 (cycloaliphatic polyamine)	100:36	40 min @ 100° C	120 min @ 160° C
H3585/2954	Huntsman XB 3585 (epoxy)	Huntsman Aradur 2954 (cycloaliphatic polyamine)	100:33	40 min @ 100° C	120 min @ 160° C
H8615/8615	Huntsman Araldite LY 8615 (epoxy)	Huntsman Aradur 8615, (cycloaliphatic polyamine)	100:50	40 min @ 100° C	60 min @ 150° C, 60 min @ 180° C
H1560/917/070	Huntsman Araldite 1560 (epoxy)	Huntsman Aradur LY 917 (anhydride hardener) + Accelerator DY 070 (imidazole accelerator)	100:118:0.25 (Resin: Hardener: Accelerator)	30 min @ 130° C	240 min @ 180° C

Neat Resin Specimen Manufacture

Neat resin specimens were manufactured from the same resins as the composites, as described in Table 1. Resin pre-heating, mixing, curing, and post-curing followed the same procedures as for the composites. Resins were cast by pouring the pre-heated resin into a mostly closed mold with one open edge at the top. Coupons were cut from the resin sheets using a diamond bladed wet saw.

Dynamic Mechanical Analysis and Thermogravimetric Analysis

Composites were tested following ASTM D7028 in three-point bending on a DMA (TA Instruments, DMA Q800) at 1 Hz to a maximum strain of 0.1%. The temperature was ramped at 10° C/min from 25° C to the maximum temperature in a nitrogen environment. T_g was recorded using a step transition analysis of the storage modulus. Dry sample DMA tests were conducted on samples dried in an oven at 100° C for 2 hours prior to testing to remove any absorbed moisture. Wet sample DMA tests were conducted on samples placed in Dex-Cool engine coolant (Zerex 50/50, 50% water and 50% ethylene glycol) at 95° C for 2 weeks. Composite samples were also tested by TGA (Mettler Toledo, Model TGA 1) from 25-600° C at a heating rate of 10° C/min in an air environment to assess thermal stability.

Mechanical Testing

Mechanical testing was conducted on a 150 kN Universal Testing Machine (Instron, Model 5984) equipped with an environmental chamber (Instron, Model 3119-610). Samples were tested in tension, compression, short beam shear, and flexure. In general, samples failed in a brittle manner with a sudden drop in load. However, some tests at high temperature resulted in ductile

failure modes that were not abrupt and the test was ended manually to prevent damage to fixturing. Unless otherwise noted, four tests were conducted under each condition and error bars were generated based on the standard deviation of the data.

- Tensile tests were run according to ASTM D3039 on samples nominally measuring 254 mm long by 36 mm wide by 2.7 mm thick. Samples were un-tabbed and had a gage length of 152 mm. Load was applied using manual wedge grips under displacement control at 4 mm/min to failure and measured using a 150 kN load cell. Strain was measured using a 50 mm gage length clip-on extensometer (Instron, Model 2630-112).
- Compression tests were run according to ASTM D6641 on samples nominally measuring 152 mm long by 36 mm wide by 2.7 mm thick. Samples were un-tabbed and had a gage length of 25 mm. Load was applied using a specialized fixture described in the standard (Combined Loading Compression Fixture) under displacement control at 1.5 mm/min to failure and measured using a 150 kN load cell. Strain was not measured.
- Short beam shear tests were run according to ASTM D2344 on samples nominally measuring 16 mm long by 36 mm wide by 2.7 mm thick. The span of the fixture was 11 mm. Load was applied using a three-point bending fixture under displacement control at 1 mm/min to failure and measured using a 150 kN load cell. Short beam shear tests do not yield a measure of modulus.
- Flexure tests were run according to ASTM D2344 on samples nominally measuring 80 mm long by 36 mm wide by 2.7 mm thick. The span of the fixture was 65 mm (span:thickness ratio = 24:1). Load was applied using a three-point bending fixture under displacement control at 4 mm/min to failure and measured using a 5 kN load cell. Strain was measured according to the standard using cross-head displacement as the measure for cross-head displacement.

In many cases it is useful to compare the relative change in properties as a function of temperature from one material to another. In these cases, data was normalized by dividing the material property at a given temperature by the material property at room temperature. This value is defined as the “retained” property; for example, “retained flexural modulus”.

Long-Term Exposure

Composites were exposed to a variety of long-term elevated temperature conditions then tested to measure residual mechanical performance. Media and temperature in each case was chosen to simulate conditions that would be experienced by a composite in under-the-hood applications. In all cases, 80 mm long by 36 mm wide by 2.6-2.8 mm thick (thickness varied from sample to sample) were conditioned and then tested in flexure. Samples exposed to hot air were treated in a mechanical convection oven, *i.e.* air in the oven was circulated by a fan (Despatch, Model RFD2-19-2E). Air was continuously vented and replenished in the oven. Samples were placed in the oven on a wire rack to minimize covered surfaces. Samples exposed to engine coolant (Zerex 50/50, 50% water and 50% ethylene glycol) were treated in a continuously circulated heated bath (Julabo, Model F26-HE) at 95° C. The engine coolant was composed of 50% ethylene glycol and 50% water, with small amounts of other additives. Samples were placed in the bath in such a way as to provide free-space between each. Samples exposed to engine oil (Mobil 5W-30) were treated in a continuously circulated heated bath at 150° C. Mass of each sample was periodically measured on a high precision scale (+/- 0.0001 g accuracy) to evaluate degradation of the epoxy or uptake of the conditioning media.

Results and Discussion

DMA Test Results

The T_g is among the most important values dictating the performance of a polymer as a function of temperature. DMA tests are often conducted to assess the T_g of a polymer or

composite as well as get a continuous measure of the material's stiffness over a range of temperatures by using a temperature sweep. For strain-rate insensitive materials, storage modulus gives a good estimate of how the material's structural stiffness will change with temperature. It is important to keep in mind that the change in storage modulus of a neat resin does not directly relate to the change in modulus of a composite, since the fibers generally dominate the stiffness in a composite.

DMA tests were conducted on each of the resins using a temperature sweep at a constant ramp rate. Results are shown in Figure 2, with the various measures of T_g tabulated in Table 2. Overall, all five polymers behaved similarly. All polymers had similar storage modulus at the cold starting temperature of approximately 3 GPa. D383/BV-ME-PS2 and H1560/917/070, the two anhydride cured systems, showed the most stable storage modulus in the glassy region. H3585/2954 and H8615/8615 showed secondary local peaks in the loss modulus corresponding to a sudden drop in storage modulus well below T_g. This behavior often indicates under-curing of the resin and post-curing during the test. The highest T_g's were measured in H8615/8615 and H1560/917/070 at over 200° C by all three measures. H3585/2954 and D383/BV-ME-PS2 were in the 160-180° C range and H3598/2954 in the 140-160° C range. Storage modulus onset provides the lowest measure, which generally makes it the most conservative when setting service temperature. Tan(δ) was the highest. Unless otherwise noted, this report will refer to the storage modulus onset temperature as the T_g.

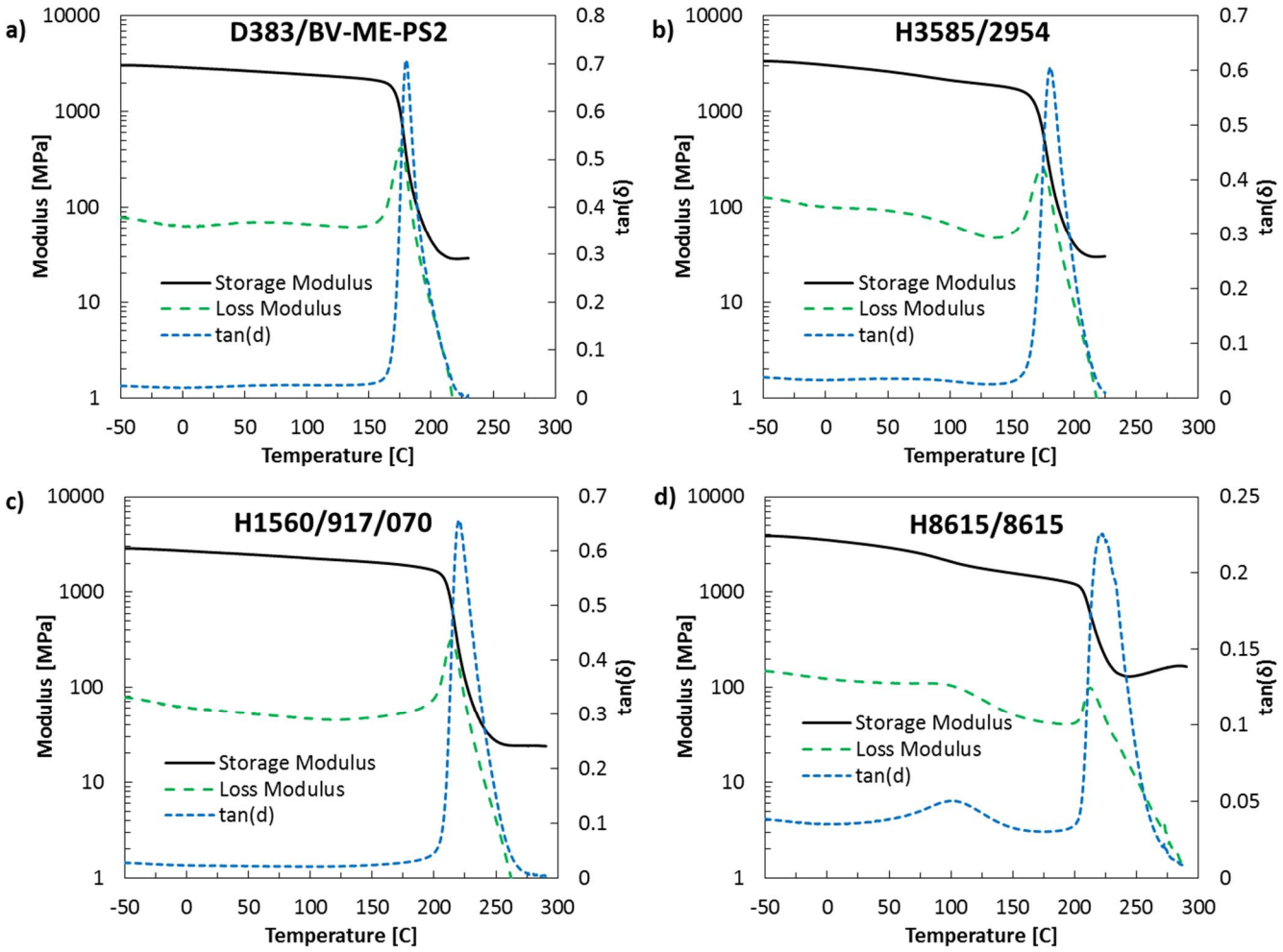

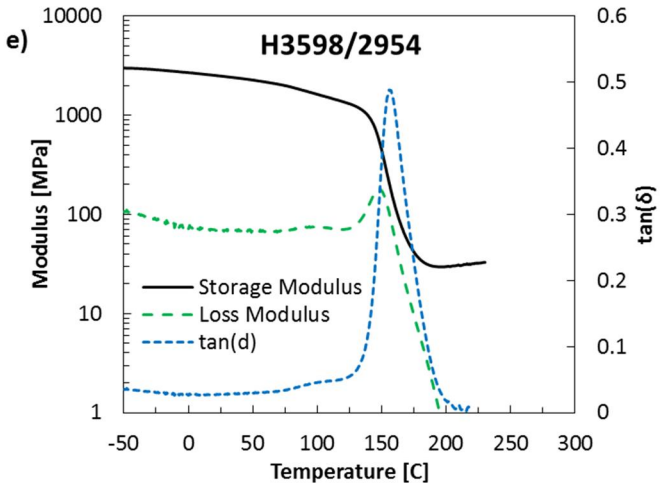

Figure 2: DMA data for each resin, including storage modulus, loss modulus, and tan(δ).

Table 2: Summary of T_g values as measured by DMA for the different materials as shown in Figure 2.

	Storage Modulus Onset [°C]	Loss Modulus Peak [°C]	tan(**δ**) Peak [°C]
D383/BV-ME-PS2	168	176	180
H3598/2954	143	147	156
H3585/2954	163	174	180
H8615/8615	205	212	221
H1560/917/070	206	214	219

Tensile, Compression, Short-Beam Shear, and Flexure Comparison

Results from tensile, compression, short-beam shear (SBS), and flexure tests are shown in terms of property retention at 120° C in Figure 3 and non-normalized values in Table 3 and Table 4. A temperature of 120° C was chosen as a representative temperature for under-the-hood exposure. In general, the strength of the composite was much more sensitive to temperature than the modulus. Both tensile and flexural modulus was nearly unchanged at 120°C, in most cases, while the strength dropped for all resins in flexure, SBS, and compression. The exception to the observation above is that the tensile strength was mostly insensitive to temperature and even increased slightly in all cases except for H3598/2954. In the case of H3598/2954, 120° C was significantly closer to the resin's T_g of 143°C than the other resins. The next closest T_g was for H3585/2954 at 163° C; 43° C above the test temperature. Flexure, SBS, and compression all showed similar sensitivities to temperature. SBS was a bit less sensitive for some resins, notably H3598/2954 and H3585/2954. Flexure and compression showed very similar behavior, indicating that flexure is a good stand in test for compression when looking at the temperature sensitivity of a matrix material, since flexure tests are easier to run and require less material. However, the non-normalized compressive strength is much lower than the non-normalized flexure strength. Therefore, flexure can estimate the drop in compressive strength with temperature, but not the actual compressive strength in the absence of any baseline compression strength data.

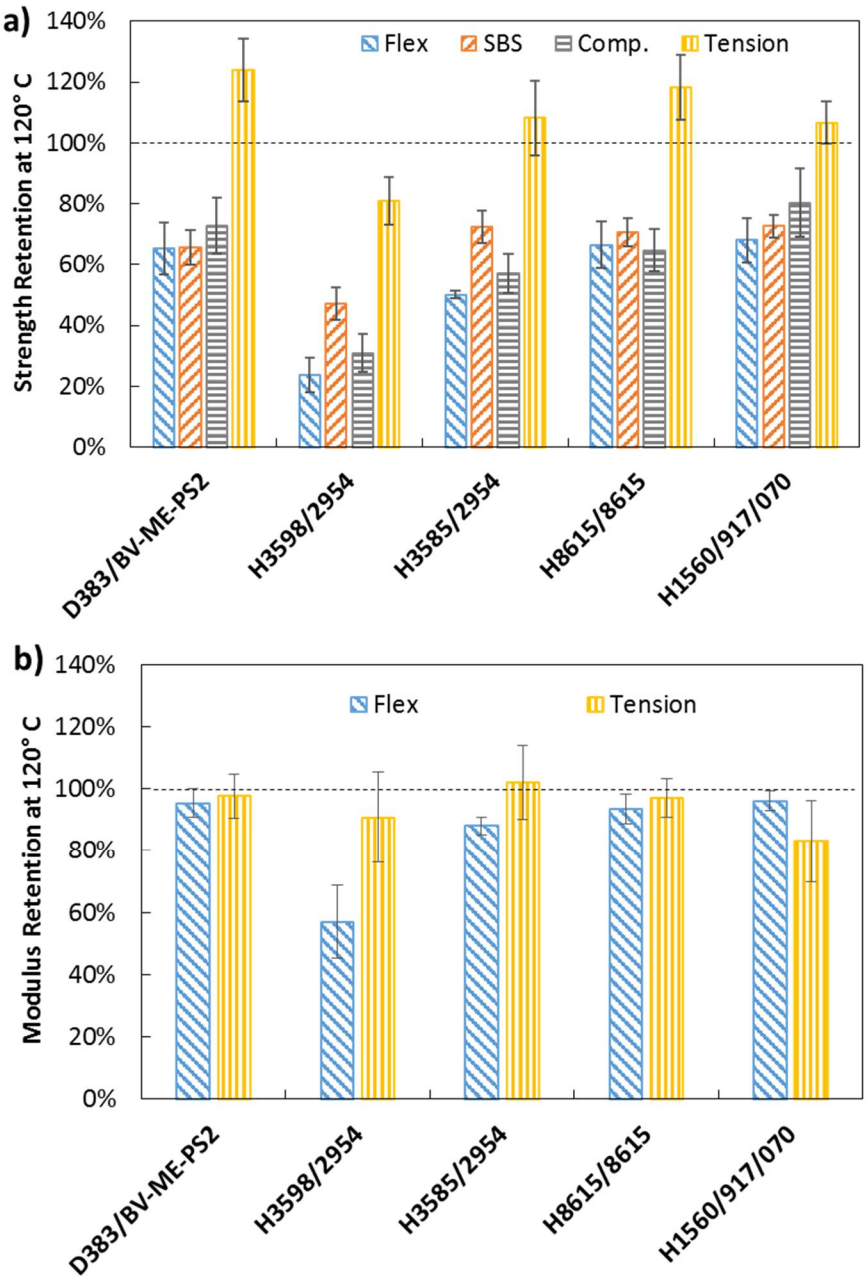

Figure 3: (a) Retained strength and (b) retained modulus for each resin when tested in flexure, SBS, compression, and tension. Error bars represent one standard deviation. Modulus was not measured for compression data. Short beam shear tests do not yield a measure of modulus. Refer to Table 3 and Table 4 for non-normalized data.

Table 3: Non-normalized strength results for various tests of each material system as shown in Figure 3a. Values are provided as MPa.

Resin	Test Mode	23°C	120°C	Retention
D383/BV-ME-PS2	Flex	756 ± 63	494 ± 24	65 ± 9 %
D383/BV-ME-PS2	SBS	44.6 ± 2.4	29.3 ± 1.4	66 ± 6 %
D383/BV-ME-PS2	Comp.	399 ± 36	290 ± 8	73 ± 9 %
D383/BV-ME-PS2	Tension	665 ± 53	824 ± 35	124 ± 10 %
H3598/2954	Flex	673 ± 38	160 ± 8	24 ± 6 %
H3598/2954	SBS	42.7 ± 2.2	20.1 ± 1.4	47 ± 5 %
H3598/2954	Comp.	417 ± 26	129 ± 17	31 ± 6 %
H3598/2954	Tension	837 ± 60	676 ± 33	81 ± 8 %
H3585/2954	Flex	814 ± 7.0	408 ± 17	50 ± 1 %
H3585/2954	SBS	41.3 ± 2.0	29.9 ± 1.2	72 ± 5 %
H3585/2954	Comp.	445 ± 26	254 ± 18	57 ± 6 %
H3585/2954	Tension	733 ± 75	793 ± 46	108 ± 12 %
H8615/8615	Flex	725 ± 42	482 ± 55	66 ± 8 %
H8615/8615	SBS	36.2 ± 1.6	25.6 ± 0.7	71 ± 5 %
H8615/8615	Comp.	388 ± 25	251 ± 16	65 ± 7 %
H8615/8615	Tension	580 ± 42	686 ± 38	118 ± 11 %
H1560/917/070	Flex	824 ± 56	560 ± 32	68 ± 7 %
H1560/917/070	SBS	43.0 ± 1.6	31.2 ± 0.5	73 ± 4 %
H1560/917/070	Comp.	386 ± 39	310 ± 24	80 ± 11 %
H1560/917/070	Tension	728 ± 50	776 ± 7	107 ± 7 %

Table 4: Non-normalized testing results for flexural and tensile modulus as shown in Figure 3b. Values are given in GPa.

Resin	Test Mode	23°C	120°C	Retention
D383/BV-ME-PS2	Flex	41.5 ± 0.4	39.6 ± 1.9	95 ± 4 %
D383/BV-ME-PS2	Tension	46.7 ± 1.7	45.6 ± 2.9	98 ± 7 %
H3598/2954	Flex	38.8 ± 0.4	22.1 ± 0.8	57 ± 12 %
H3598/2954	Tension	43.0 ± 3.3	39.0 ± 5.9	91 ± 15 %
H3585/2954	Flex	40.2 ± 0.9	35.4 ± 0.8	88 ± 3 %
H3585/2954	Tension	46.8 ± 1.3	47.8 ± 5.3	102 ± 12 %
H8615/8615	Flex	39.8 ± 0.5	37.2 ± 2.0	93 ± 5 %
H8615/8615	Tension	47.0 ± 2.4	45.6 ± 1.6	97 ± 6 %
H1560/917/070	Flex	41.5 ± 1.0	39.9 ± 0.9	96 ± 3 %
H1560/917/070	Tension	46.5 ± 2.0	38.6 ± 1.9	83 ± 13 %

A detailed assessment of the effect of temperature on the flexural strength and modulus of all matrix resins is shown normalized in Figure 4 and non-normalized in Table 5. In addition, the plots include tensile data from a cast aluminum alloy for comparison of property retention (flexure data was unavailable). For all composites, the strength decreased fairly linearly as temperature increased. Also, in general, the higher the T_g, the higher the strength retention at a given temperature. In contrast, the modulus was mostly steady well below T_g before dropping precipitously when approaching T_g. Close inspection shows that this drop actually occurred below T_g for all resins but generally corresponded with T_g; *i.e.*, as T_g increased so did the point of the

drop. H8615/8615 and H1560/917/070 had the highest T_g, equal to about 205° C, and reached much higher temperatures than the other resins before losing significant modulus. Interestingly, the modulus of H1560/917/070 dropped before H8615/8615 despite the two resins having similar T_g. In fact, T_g was not fully indicative of the performance at a given temperature for either strength or modulus. For example, comparison of D383/BV-ME-PS2 (T_g = 168° C) and H3585/2954 (T_g = 163° C) show significant differences in performance at elevated temperature despite T_g values differing by only 3%.

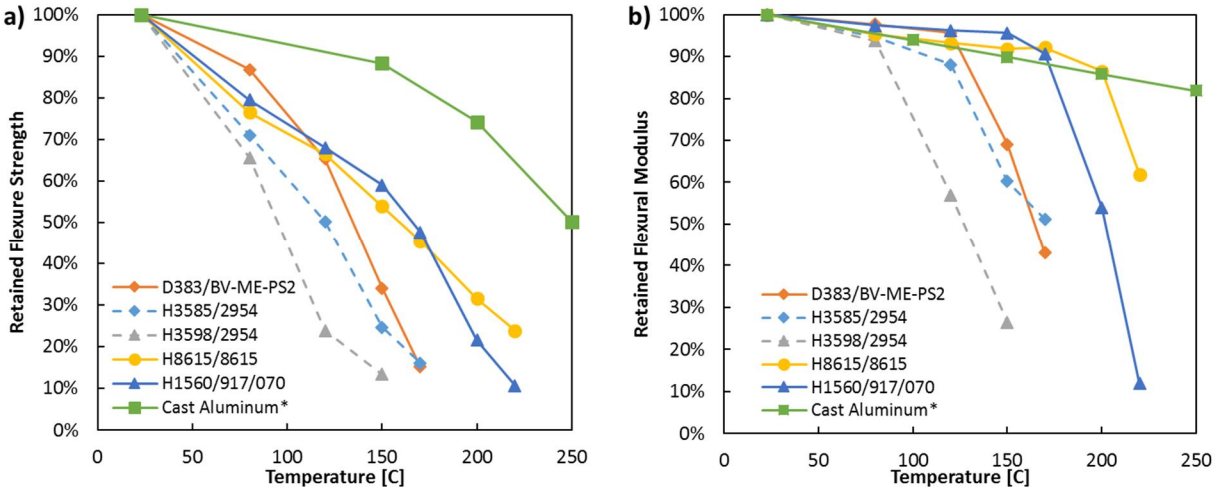

Figure 4: (a) Retained flexural strength and (b) retained flexural modulus for each resin evaluated as a function of temperature. Tensile testing data for high pressure die cast aluminum) is included for general comparison of property retention between aluminum and the composite materials as a function of temperature. No error bars are included on this graph for improved clarity; refer to Table 5 for non-normalized data with error bars included.

The rough comparison of aluminum tensile properties to composite flexure properties shows that the aluminum also loses more strength at a given temperature than modulus, but retains higher performance than the composites. However, similar modulus retention is observed for aluminum and the composites when the composite is well below T_g of the given matrix.

The importance of T_g to the mechanical performance of the material is better visualized when evaluating the modulus and strength as a function of test temperature (T) minus material T_g (Figure 5). This shifting of the curves is based on the time–temperature superposition principle for viscoelastic materials. By plotting as a function T-T_g, the retained flexural modulus curves of each of the epoxy resins begin to largely overlap. The shape of the curves is largely the same for each resin, indicating that the only major difference between them with respect to the dependence of modulus on temperature is the T_g. The only outlier is H8615/8615 at temperatures above T_g. The higher retained modulus at elevated temperatures for this system is likely indicative of the large number of multifunctional groups in this resin system that cause a very high level of cross-linking and the resulting high T_g. Notably, the drop off in modulus for all of the resins initiates approximately 50° C below T_g. This likely relates to the “rule-of-thumb” common in the aerospace industry that the service temperature of an epoxy resin should be set at 50° C below T_g. In terms of strength, the curves appear to overlap near T_g, but differ significantly well below T_g. The time–temperature superposition principle does not apply to strength and therefore it is not surprising that the curves don’t show the same overlapping behavior as the result of shifting.

Table 5: Non-normalized flexure testing results for the data shown in Figure 4. The failure type was subjectively determined based on the shape of the stress-strain curve and the level of plasticity exhibited.

Resin	Temp [C]	Flex Strength [MPa]	Flex Strength Retention	Flex Modulus [GPa]	Flex Modulus Retention	Failure Type
D383/BV-ME-PS2	23	756 ± 63	-	41.5 ± 0.4	-	Brittle
D383/BV-ME-PS2	80	656 ± 23	87%	40.5 ± 1.4	98%	Brittle
D383/BV-ME-PS2	120	494 ± 24	65%	39.6 ± 1.9	96%	Brittle
D383/BV-ME-PS2	150	258 ± 29	34%	28.6 ± 3.2	69%	Ductile
D383/BV-ME-PS2	170	115 ± 14	15%	17.9 ± 5.3	43%	Ductile
H3598/2954	23	673 ± 38	-	38.8 ± 0.4	-	Brittle
H3598/2954	80	441 ± 36	66%	36.4 ± 1.2	94%	Brittle
H3598/2954	120	160 ± 8	24%	22.1 ± 0.8	57%	Ductile
H3598/2954	150	90 ± 9	13%	10.3 ± 0.5	26%	Ductile
H3585/2954	23	814 ± 7	-	40.2 ± 0.9	-	Brittle
H3585/2954	80	578 ± 21	71%	38.1 ± 1.9	95%	Brittle
H3585/2954	120	408 ± 17	50%	35.4 ± 0.8	88%	Brittle
H3585/2954	150	201 ± 54	25%	24.2 ± 2.6	60%	Ductile
H3585/2954	170	131 ± 20	16%	20.6 ± 4.1	51%	Ductile
H8615/8615	23	725 ± 42	-	39.8 ± 0.5	-	Brittle
H8615/8615	80	554 ± 25	76%	38 ± 1.7	95%	Brittle
H8615/8615	120	482 ± 55	66%	37.2 ± 2	93%	Brittle
H8615/8615	150	391 ± 44	54%	36.6 ± 1.4	92%	Brittle
H8615/8615	170	329 ± 42	45%	36.7 ± 1.5	92%	Brittle
H8615/8615	200	229 ± 13	32%	34.5 ± 0.9	87%	Brittle
H8615/8615	220	173 ± 40	24%	24.7 ± 4	62%	Brittle
H1560/917/070	23	824 ± 56	-	41.5 ± 1	-	Brittle
H1560/917/070	80	655 ± 37	80%	40.4 ± 1.7	97%	Brittle
H1560/917/070	120	560 ± 32	68%	39.9 ± 0.9	96%	Brittle
H1560/917/070	150	486 ± 23	59%	39.6 ± 0.6	96%	Brittle
H1560/917/070	170	392 ± 24	48%	37.6 ± 0.6	91%	Brittle
H1560/917/070	200	177 ± 31	22%	22.4 ± 2.1	54%	Brittle
H1560/917/070	220	88 ± 4	11%	4.9 ± 2.8	12%	Ductile

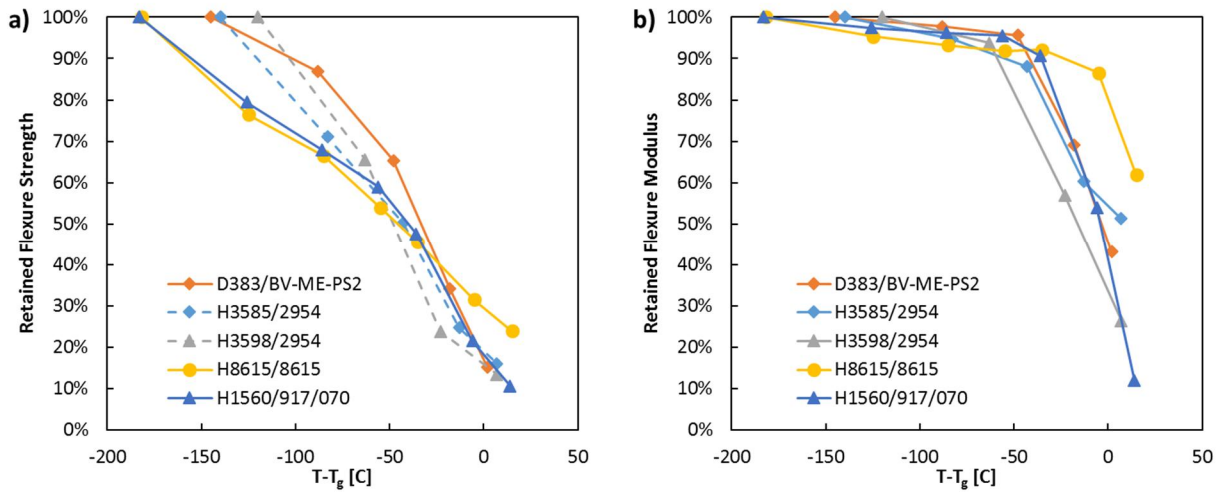

Figure 5: (a) Retained flexural strength and (b) retained flexural modulus for each resin evaluated as a function of test temperature minus material glass transition.

Failure Mode Analysis

As discussed, increasing the temperature of the composite causes the matrix to undergo a transition from glassy to rubbery near the T_g. In the last section, this was shown to correspond to a dramatic loss in composite modulus near T_g. In addition, this transition also alters the failure mode. Figure 6-Figure 9 show representative data curves and failure mechanisms for flexure, compression, SBS, and tension, respectively. In all cases, data and images for the H3598/2954 system are shown because it is the only resins to show brittle-type failures at room temperature and ductile-type failures at 120° C. All other resins had a higher T_g and failed in a brittle manner at both temperatures.

Figure 6 shows the results for flexure at all four tested temperatures, as well as the compression side of representative samples after testing. At 23°C and 80°C, the stress increased linearly with strain before sharp compression cracks were observed to form in the composite and the stress decreased in a jagged manner. The post-testing image in Figure 6b shows the brittle-type crack that formed on the compression-side. In contrast, at 120°C and 150°C the stress-strain curve was only linear for a short period before curving gradually to signal a large amount of plasticity in the material. As expected, Figure 6c shows significant plastic deformation on the compressive surface in the form of what appears as “bubbling.” In actuality, these are small areas of microbuckling of the material under plastic deformation. Note, the absence of a sharp crack. Table 5 includes categorization of the failure mode for each resin at each tested temperature. All resins showed a transition from brittle to ductile failure near T_g, with the exception of H8615/8615. This resin did show significant reduction in mechanical performance through 220°C, but still failed in a brittle manner.

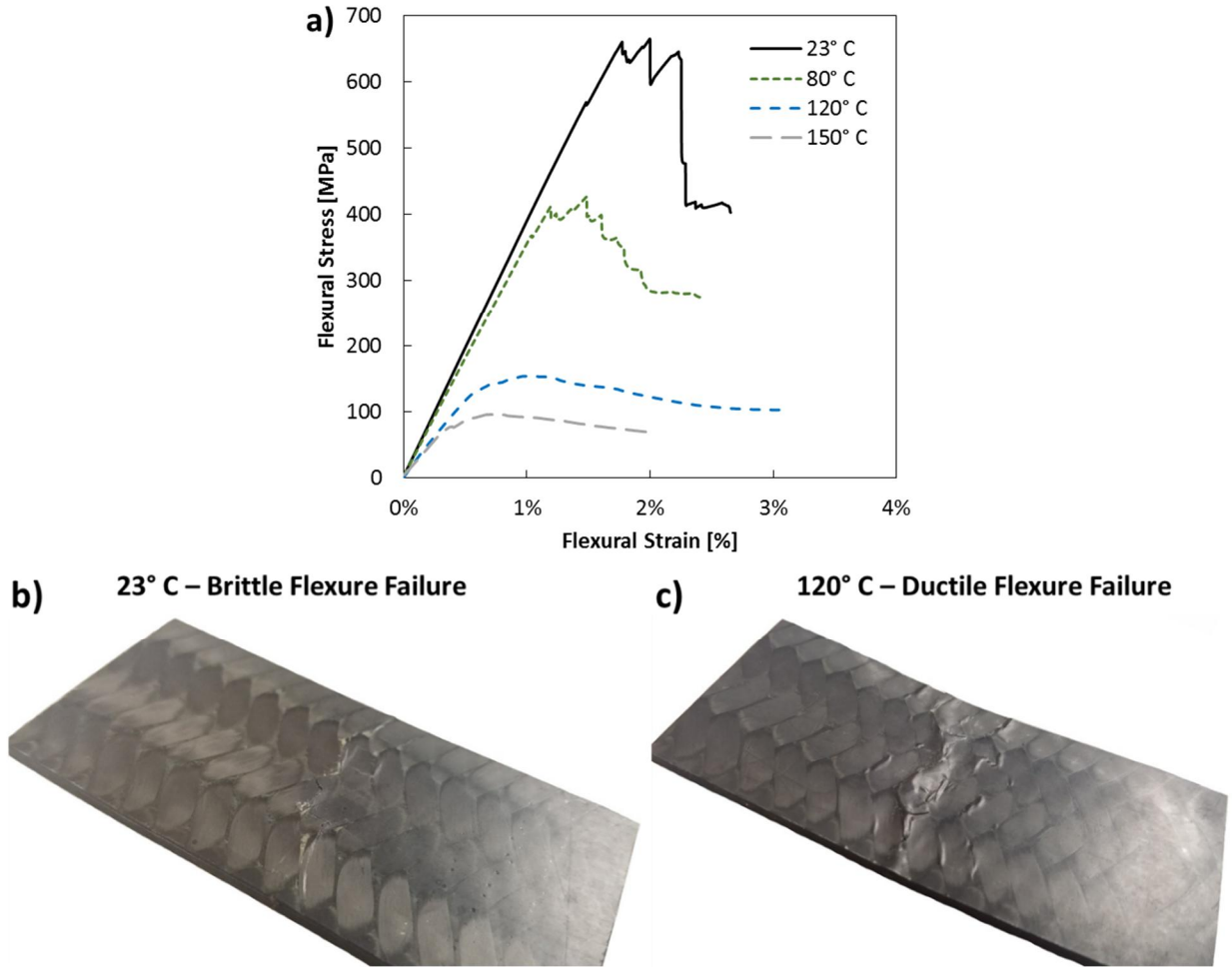

Figure 6: (a) Representative test data curves for flexure tests at various temperatures. (b) An example of a sample with a brittle-type failure showing a sharp crack. (c) An example of a sample with a ductile-type failure showing a large amount of plastic deformation resulting in a wrinkled appearance. Test data and samples are from tests on H3598/2954 and are representative of the types of curves and failure modes observed for all five resins. Samples measured approximately 36 mm wide by 80 mm long by 2.7 mm thick.

Compressive stress-extension curves and representative failure modes are shown in Figure 7. Unlike flexure, the data curve was fairly linear at both 23°C and 120°C before failing suddenly. The non-linearly observed at 23°C is likely due to the compliance of the fixturing, resulting in additional extension being measured and not representative of the material behavior. This compliance would be removed if material strain has been directly measured rather than plotting the stress as a function of cross-head extension. Post-failure photographs show brittle failure at 23°C characterized by extensive shear cracking and brooming. At 120°C, two failure modes were observed. One was a ductile failure characterized by localized plastic microbuckling of the sample. In the second, the same type of brittle failure mode occurred that was observed at 23°C. The same stress-extension behavior was observed for both failure modes. The two types of failure modes, one brittle and one ductile, is likely due to the proximity of the test to the material's T_g. As shown in Figure 4, near T_g the material loses modulus very rapidly with increased temperature. This has the effect of making the failure mode very sensitive to temperature.

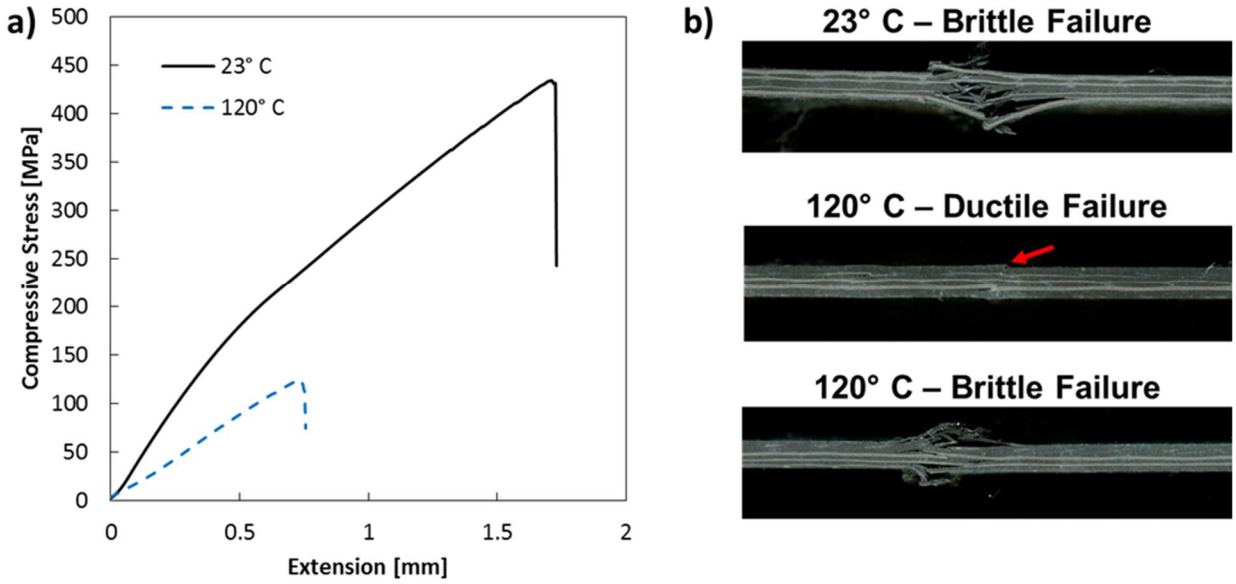

Figure 7: (a) Representative test data curves for compression tests at two temperatures. Note that the measure of crosshead extension includes slip in the fixture and is therefore not fully representative of material response. (b) Examples of various failure modes, including brittle-type failure at 23°C, a ductile failure at 120°C and a brittle failure at 120°C. Test data and samples are from tests on H3598/2954 and are representative of the types of curves and failure modes observed for all five resins. The arrow in the second image indicates the failure location. Samples measured approximately 36 mm wide by 152 mm long by 2.7 mm thick.

Figure 8 gives the results and failure modes from SBS testing. As observed in the other test modes, a brittle-type behavior is seen at 23°C and a ductile-type behavior at 120°C. The brittle failure occurred suddenly after a linear increase in stress. In contrast, at elevated temperature the sample deformed plastically and never catastrophically failed.

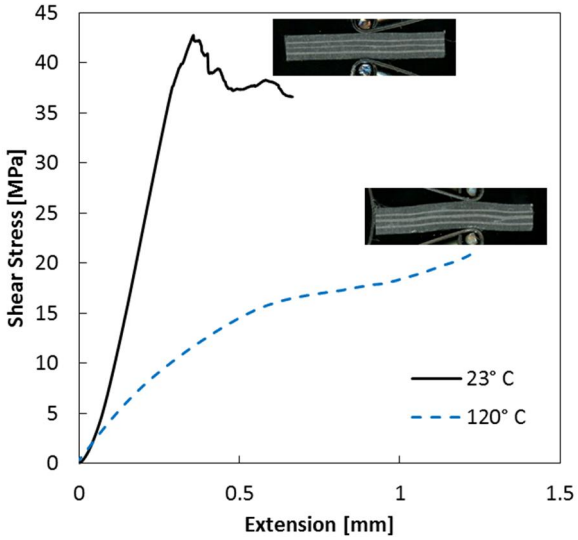

Figure 8: Representative test data curves for short beam shear tests at two temperatures. Example of sample deformation after testing are shown, including a sample that experienced brittle-type failure at 23°C and one that experiences ductile failure at 120°C. Test data and samples are from tests on H3598/2954 and are representative of the types of curves and failure modes observed for all five resins. Samples measured approximately 36 mm wide by 16 mm long by 2.7 mm thick.

The tensile behavior of the composite at 23°C and 120°C is shown in Figure 9. At both temperatures the stress increased linearly with strain before sudden and catastrophic failure of the material. As noted previously, the failure stress and modulus were relatively unaffected by the temperature compared with the other modes. Post-failure images show that the failure modes were similar at both temperatures with failure caused by fiber breakage. This explains the insensitivity of tensile performance to temperature since the fiber properties are much less sensitive to temperature than the matrix.

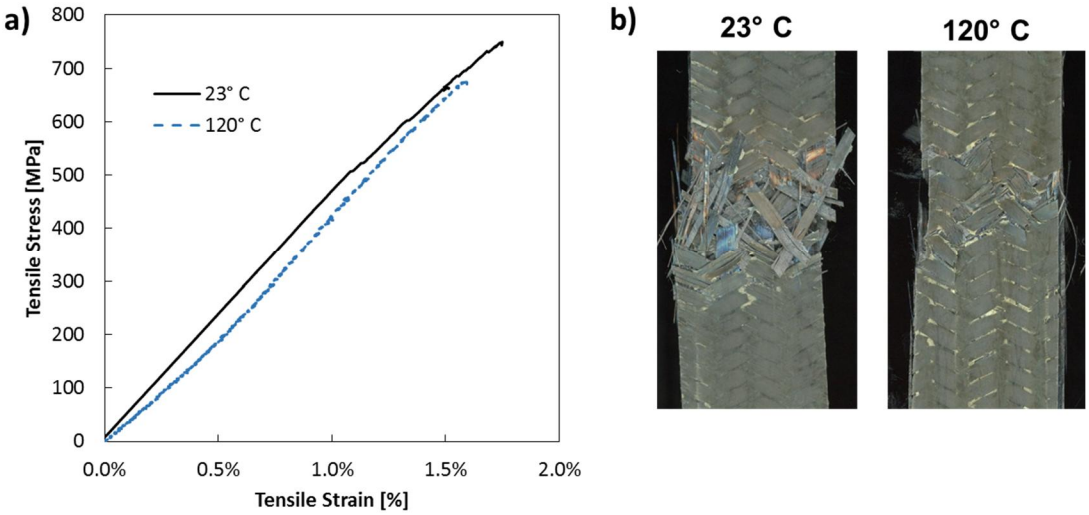

Figure 9: (a) Representative test data curves for tensile tests at two temperatures. (b) Examples of various failure modes, including failure at 23°C and at 120°C. Test data and samples are from tests on H3598/2954 and are representative of the types of curves and failure modes observed for all five resins. Samples measured approximately 36 mm wide by 254 mm long by 2.7 mm thick.

Comparison of Test Modes

Table 6 contains a general summary of the four quasi-static mechanical testing procedures discussed above for assessing the performance of a composite at elevated temperature. This table is supported by the observations previously discussed, but is subjective and meant as a starting point for choosing an appropriate test method.

Table 6: Comparison of common quasi-static mechanical testing procedures for assessing composite behavior at elevated temperature. Several categories use comparative system ranging ++ / + / - / --, with ++ being the best and -- being the worst. Note that these assessments are done subjectively based on the observations in this report.

	Flexure	Short Beam Shear	Compression	Tension
Properties Measured	Flexural: Modulus, Strength	Short Beam Strength	Compressive: Strength, Modulus (possible)	Tensile: Modulus, Strength
Dominant Failure Modes	Shear Cracking, Microbuckling	Shear Cracking	Shear Cracking, Microbuckling	Fiber Breakage
Measures a Material Property?	No	No	Yes	Yes
Ease of Test Procedure	++	+	--	-
Material Usage	+	++	-	--
Sensitivity to Temperature	++	+	++	--

High Temperature Air Exposure

Exposure to air at elevated temperature is known to oxidize composites, potentially resulting in embrittlement and mass loss. TGA was used to examine the effect of temperature over relatively short periods using a dynamic temperature sweep. Figure 10 shows the residual mass vs. temperature results. Both resins show very little mass loss below approximately 300° C. Below this point, most mass loss is likely the result of absorbed moisture or low molecular weight reactants being removed. Above approximately 300° C, mass loss accelerates to a rapid rate. D383/BV-ME-PS2 reaches 3% mass loss before H3585/2954, but then reaches 10% mass loss earlier. However, both resins show similar behavior that indicates that they should not be exposed to temperatures above 300° C for even short periods.

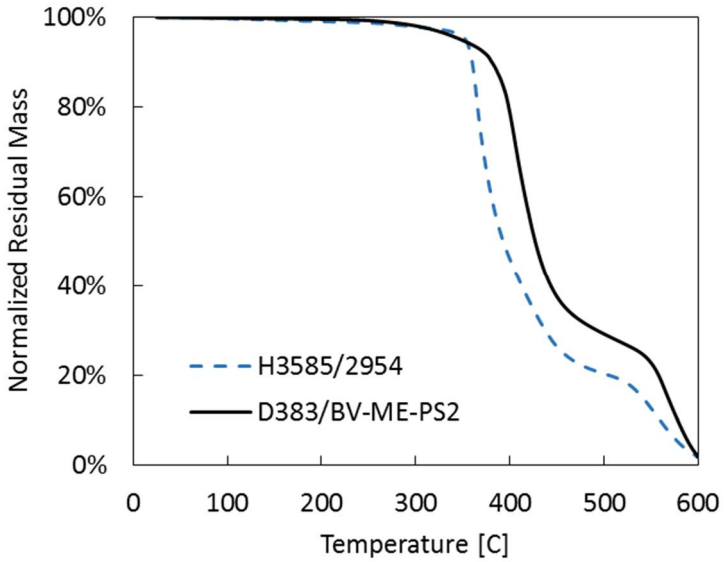

Figure 10: TGA results for two resins. Mass is normalized by dividing the residual mass at a given temperature by the starting mass.

While TGA is useful to assess short term effects of air exposure on a composite, actual composites used under-the-hood would be exposed for several thousand hours and be expected to maintain performance. Conducting such a test in a TGA would not be practical and would not yield valuable mechanical data. Flexure tests after long term exposure of composites to high temperature air was therefore necessary. Results after exposure at 150° C for up to 3000 h are shown in Figure 11 and 200° C at up to 500 h in Figure 12. Mass loss at several points was tracked and summarized in Table 7, including data from the other exposure conditions. The shorter term at 200° C reflects the fact that this is approximately 30° C above the material's T_g and therefore the composite should not be expected to perform structurally at this temperature, particularly for long periods.

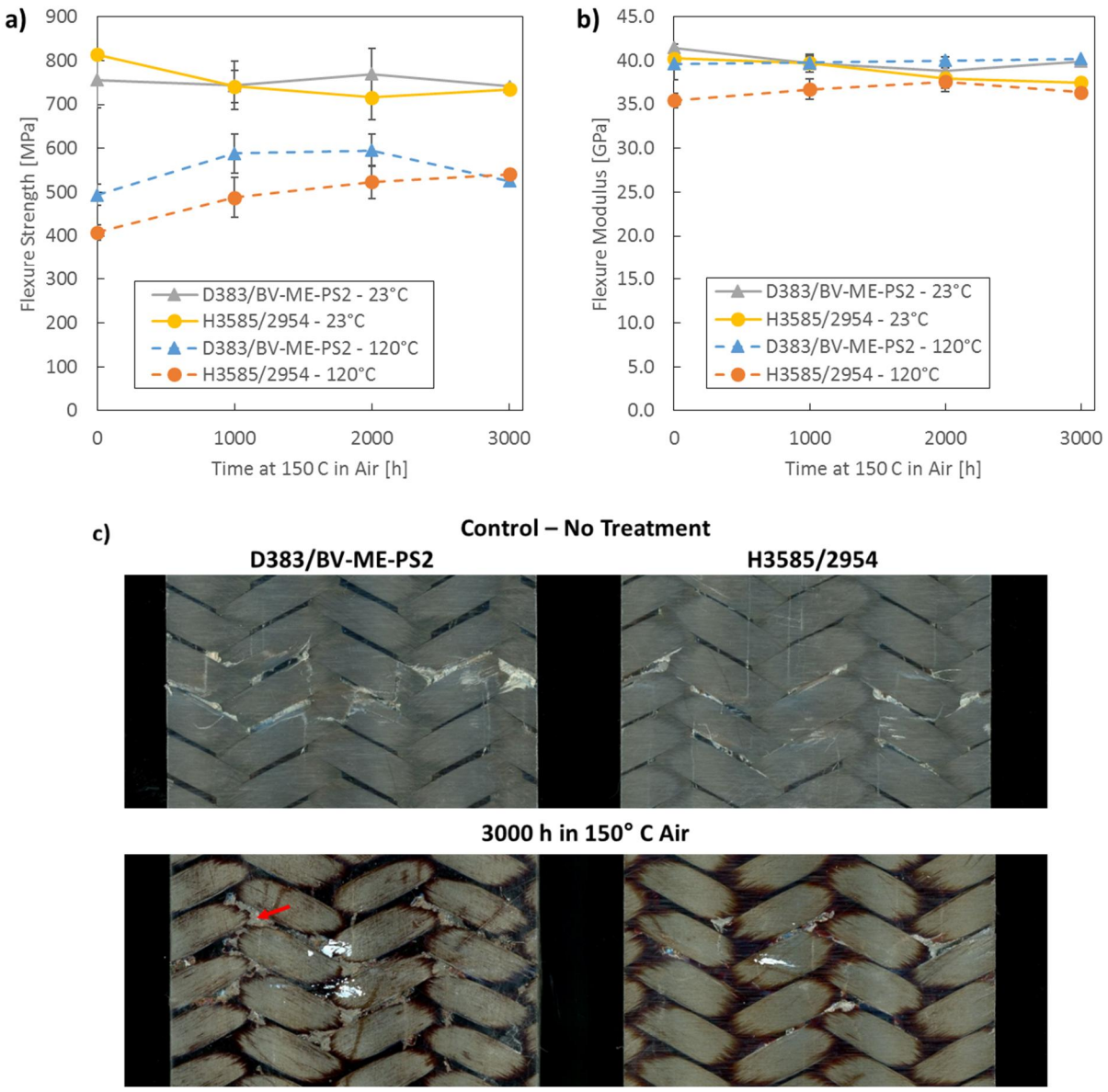

Figure 11: (a) Flexure strength and (b) flexure modulus after conditioning in 150° C air for various periods of time up to 3000 h. (c) Photographs of the sample after testing in the location of the failure on the compressive side. The arrow indicates an area where the surface resin flaked away. Photographs were taken on a document scanner (Epson Perfection V600) at 400 dpi.

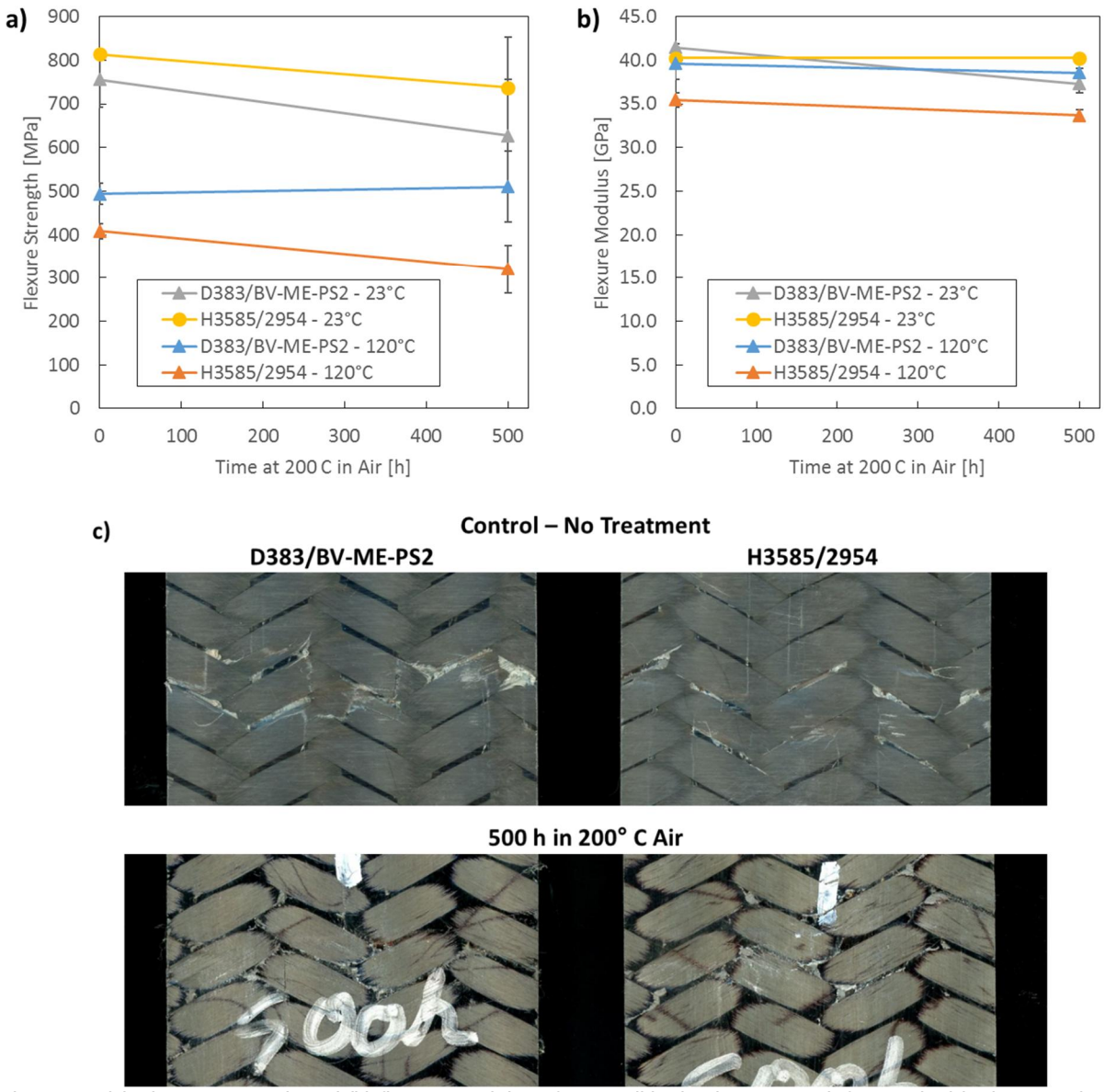

Figure 12: (a) Flexure strength and (b) flexure modulus after conditioning in 200° C air for 500 h. (c) Photographs of the sample after testing in the location of the failure on the compressive side. Photographs were taken on a document scanner (Epson Perfection V600) at 400 dpi.

Table 7: Mass change summary for each exposure condition.

Resin	Media	Temperature (° C)	Time (h)	Change
D383/BV-ME-PS2	Air	150	2000	- 0.036% ± 0.002%
D383/BV-ME-PS2	Air	200	500	- 0.477% ± 0.007%
D383/BV-ME-PS2	Oil	150	500	+ 0.060% ± 0.007%
D383/BV-ME-PS2	Dexcool	95	500	+ 0.380% ± 0.013%
H3585/2954	Air	150	2000	- 0.278% ± 0.023%
H3585/2954	Air	200	500	- 1.090% ± 0.026%
H3585/2954	Oil	150	500	- 0.103% ± 0.020%
H3585/2954	Dexcool	95	500	+ 0.543% ± 0.069%

Tests performed at both 23° C and 120° C on composites exposed to 150° C for up to 3000 h show no degradation in flexural strength or modulus. Interestingly, it appears that there was a slight increase in 120° C performance after long-term exposure, which indicates some post-curing of the material. Visually, both matrix materials were significantly darkened after 3000 h at 150° C. In the failure region, it appears that the surface resin may have embrittled since it flaked off locally in some areas. Overall, though, the failure mode remained brittle failure on the compressive side. Neither resin showed significant mass loss after 2000 h exposure, though H3585/2954 lost more mass at -0.278%, compared to -0.036% for D383/BV-ME-PS2.

Tests performed at both 23° C and 120° C on composites exposed to 200° C for up to 500 h did show some slight drop in strength, but no change in modulus. Visually, the resin darkened much more significantly and showed the same surface flaking as when the samples were exposed at 150° C. Mass loss after 500 h at 200°C was larger than after 2000 h at 150° C. Again, H3585/2954 lost more mass at -1.090%, compared with -0.477% for D383/BV-ME-PS2. Determining whether the better mass retention of D383/BV-ME-PS2 is due to being anhydride-cured or its inclusion of a thermoplastic toughening phase would require further investigation. However, anhydride-cured resins are known to be more thermally stable in general than amine-cured resins [23].

High Temperature Engine Oil Exposure

The effect of exposure of the composites to 150° C engine oil for up to 1000 h is shown in Figure 13. Much like exposure to air at 150° C, oil did not cause any measurable decrease in strength or modulus when testing the composites at 23° C and 120° C. Again, some slight post-curing may be evident for H3585/2954. Images of the sample surface again show darkening and browning of the resin. Mass change data at 500 h, shown in Table 7, actually shows a slight increase in mass in D383/BV-ME-PS2 of +0.060% and a slight decrease in mass in H3585/2954 of -0.103%. Overall, other than discoloration, oil appears to have very little effect on the composites, as would be expected for well cured epoxy resin systems.

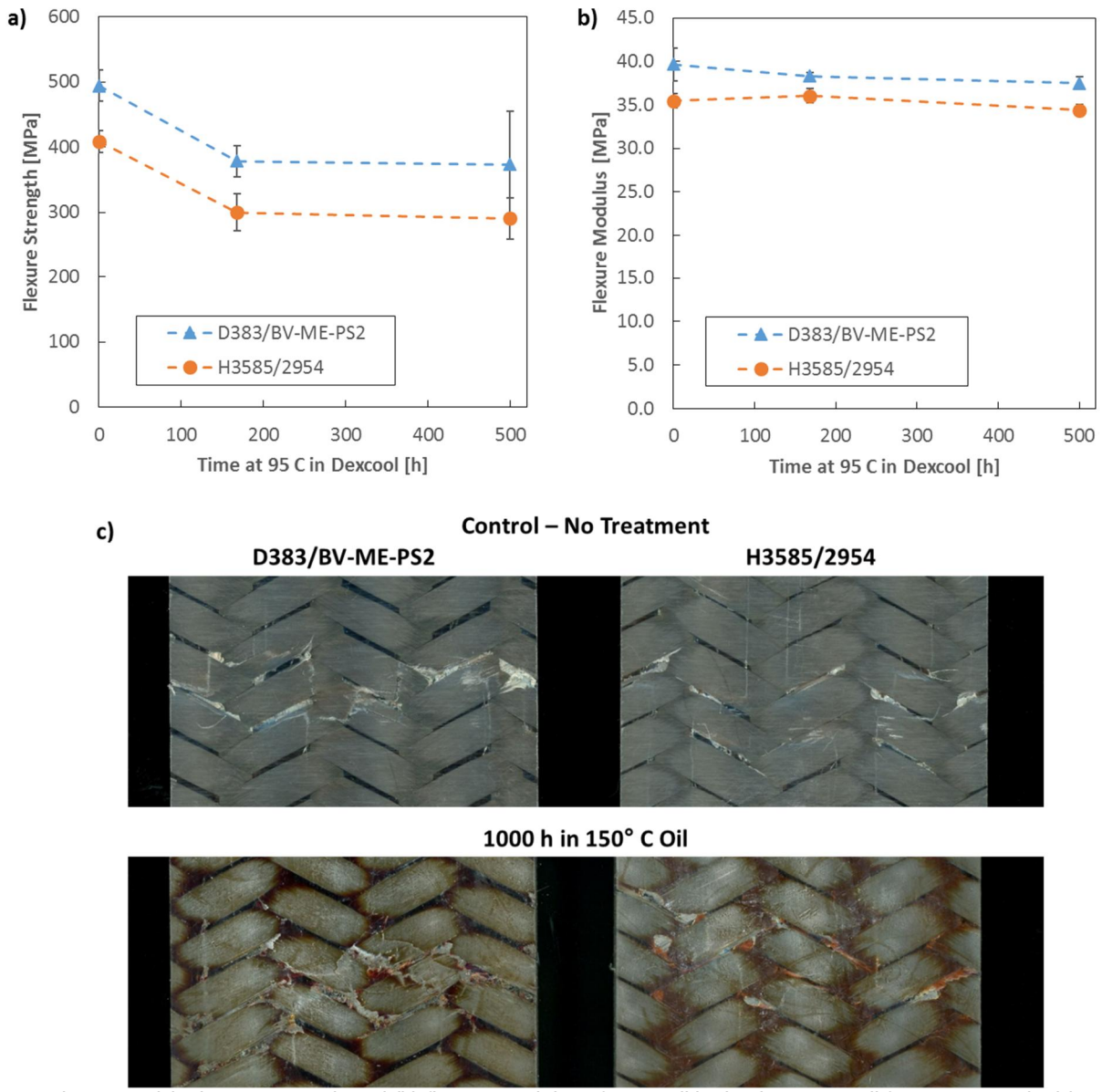

Figure 13: (a) Flexure strength and (b) flexure modulus after conditioning in 150° C oil for up to 1000 h. (c) Photographs of the sample after testing in the location of the failure on the compressive side. Photographs were taken on a document scanner (Epson Perfection V600) at 400 dpi.

High Temperature Engine Coolant Exposure

At equilibrium in standard room temperature and humidity environments, all epoxy based resins contain some level of moisture that is absorbed from the atmosphere. Additional moisture can be absorbed when submerging a composite in water leading to the potential for plasticization and reduction in elevated temperature performance.

The first assessment of the effect of engine coolant on the resin was conducted using DMA. Samples were tested before and after submersion in 95° C engine coolant for 336 hours (2 weeks). The resulting DMA curves are shown in Figure 14. In both resins, the submersion resulted in a shift in storage and loss modulus toward lower temperatures; *i.e.* the curves shifted to the left. This indicates the expected plasticization and corresponding reduction in T_g occurred. T_g was

reduced in D383/BV-ME-PS2 by 7% and in H3585/2954 by 6%. These are fairly modest but noticeable reductions.

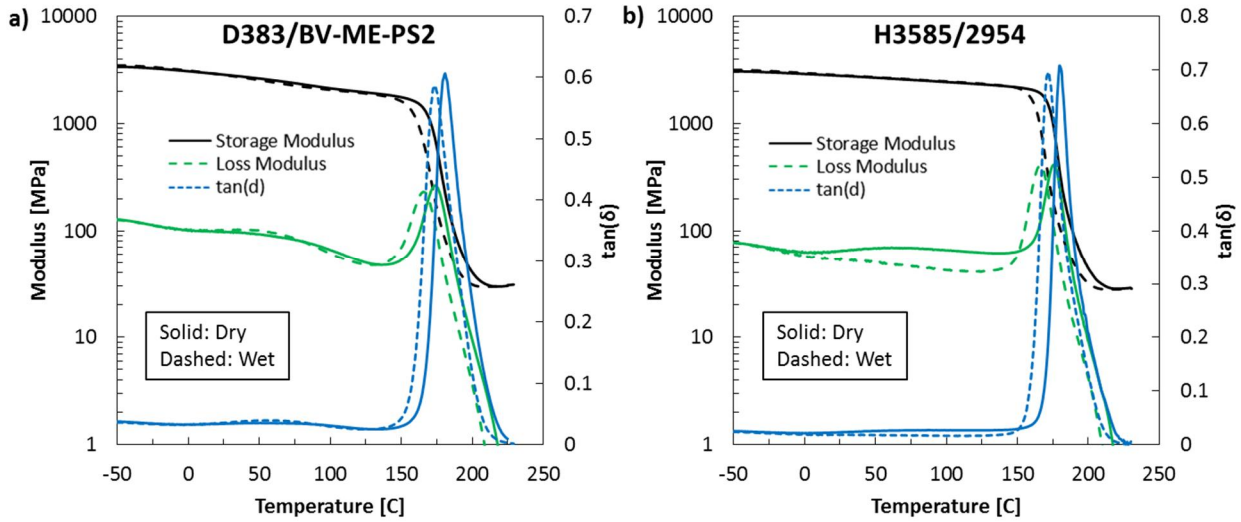

Figure 14: DMA results for two resins, (a) D383/BV-ME-PS2 and (b) H3585/2954, comparing a dry sample and a wet sample for each. In dry samples, surface moisture was removed by heating the samples in an oven prior to testing. Wet samples were placed in 95° C Dexcool for 336 hours (2 weeks) prior to testing.

The effects of exposure to 95° C engine coolant for up to 500 h on mechanical performance is shown in Figure 15. In both resins, no effect is observed in the flexural modulus at 120° C. However, the strength at 120° C was reduced significantly after just 168 h of submersion and then remained steady through 500 h. Images of the sample surface show some discolorations, particularly in D383/BV-ME-PS2, and a transition from brittle to ductile failure. Figure 16 shows the mass absorption in the two resins as a function of time submersed. Most of the mass is absorbed in the first hundred hours or so, after which the mass uptake rate slows but continues to progress. There is a much bigger jump in mass absorbed from 0 h to 168 h than from 168 h to 500 h. Comparing with the mechanical data shows that the plasticization effect has likely already occurred by 168 h and does not increase noticeably with longer exposure times or increased fluid absorption. However, more examination would be needed, including longer submersion times, to validate this. Of all of the exposure conditions examined in this study, engine coolant is the most influential to the mechanical behavior of the composite. However, it had the least effect on the visual appearance. Also, though not explicitly tested here, if this effect was due to moisture uptake, it would generally be reversible by drying out the sample [16,17].

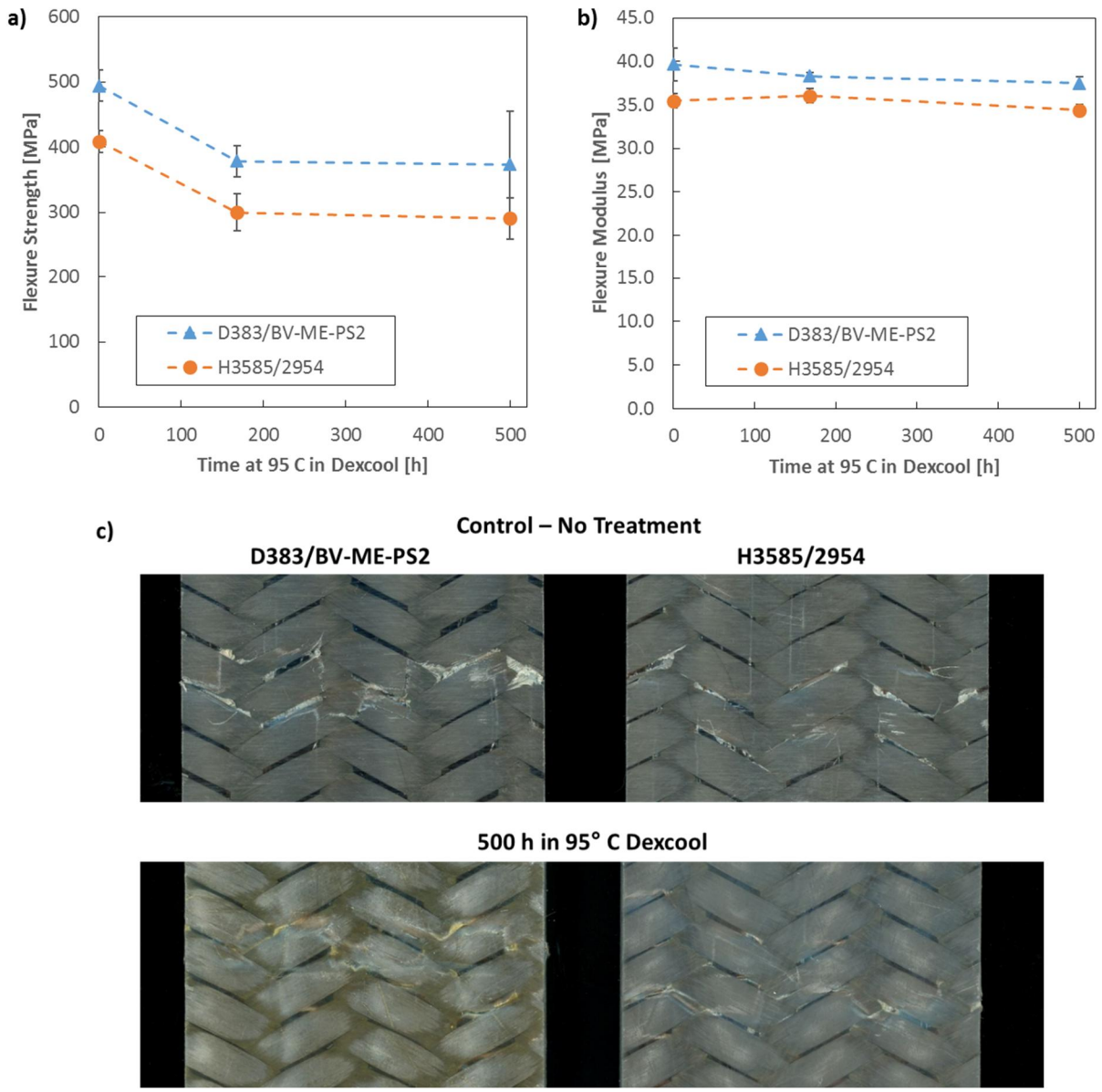

Figure 15: (a) Flexure strength and (b) flexure modulus at 120° C after conditioning in 95° C Dexcool for up to 500 h. (c) Photographs of the sample after testing in the location of the failure on the compressive side. Photographs were taken on a document scanner (Epson Perfection V600) at 400 dpi.

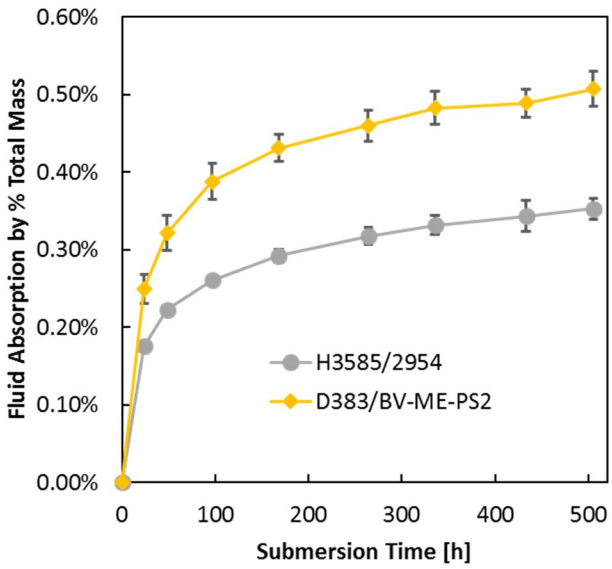

Figure 16: Fluid uptake as a function of time in 95° C Dexcool.

Conclusions

The results of this study show that epoxy-based composite materials are well suited to applications under-the-hood, but careful selection of resin is required. While glass transition temperature gives a good general indication of the performance of a resin at elevated temperature, it is not fully indicative of the actual performance at elevated temperature. In fact, two resins with the same glass transition temperature may show significant differences in performance. Service temperature as a singular number is not useful because of the varying effects of temperature on different properties of a composite. For example, if the composite will only be in tension, then it can see service at much higher temperature than if compressive stresses are present. Also, material strength properties are generally more sensitive to temperature than stiffness properties.

The effect of long term exposure to elevated temperature environments on a composite depends on the medium, extent of the temperature, and time of exposure. In 150° C air, the composite's flexural strength and modulus was unaffected at times up to 3000 hours of exposure. However, the composite matrices were visually darkened and the surface layer appeared to be embrittled. In 200° C air, the composite's flexural strength was slightly reduced after 500 h of exposure, but the modulus was unchanged. Darkening after 500 h at 200° C was more significant than after 3000 h at 150° C. Oil caused no effect on the mechanical performance of the composites when tested in flexure after up to 1000 h of exposure. However, again, significant discoloration of the resin occurred. Engine coolant caused the most significant change in mechanical performance. Flexural strength at 120° C was reduced by 20-30% after 168 h of submersion at 95°C, while flexural modulus was unaltered. The drop in strength remained consistent when the exposure time was increased to 500 h. Drops in mechanical performance due to moisture uptake are generally reversible upon heating of the composite, however, it was not evaluated in this study. Such a drop in performance would primarily be of concern after letting a vehicle sit idle for long periods of time, allowing moisture from the coolant to be absorbed.

Acknowledgements

The author would like to thank Huntsman Advanced Materials for providing samples of the resins evaluated in this study and for their technical support.

Bibliography

1. Heywood JB. Internal combustion engine fundamentals. New York: McGraw-Hill; 1988.
2. Stone R. Introduction to internal combustion engines. 3rd ed. Warrendale, Pa: Society of Automotive Engineers; 1999.
3. Mouritz AP. Fire properties of polymer composite materials. Dordrecht: Springer; 2006.
4. Mouritz AP, Feih S, Kandare E, Mathys Z, Gibson AG, Des Jardin PE, Case SW, Lattimer BY. Review of fire structural modelling of polymer composites. Compos Part Appl Sci Manuf 2009;40(12):1800–14.
5. Bausano JV, Lesko JJ, Case SW. Composite life under sustained compression and one sided simulated fire exposure: Characterization and prediction. Compos Part Appl Sci Manuf 2006;37(7):1092–100.
6. Chowdhury EU, Eedson R, Bisby LA, Green MF, Benichou N. Mechanical Characterization of Fibre Reinforced Polymers Materials at High Temperature. Fire Technol 2009;47(4):1063–80.
7. Kandare E, Kandola BK, Myler P, Edwards G. Thermo-mechanical Responses of Fiber-reinforced Epoxy Composites Exposed to High Temperature Environments. Part I: Experimental Data Acquisition. J Compos Mater 2010;44(26):3093–114.
8. Aktaş M, Karakuzu R. Determination of mechanical properties of glass-epoxy composites in high temperatures. Polym Compos 2009;30(10):1437–41.
9. Ruggles-Wrenn MB. Effects of temperature and environment on mechanical properties of two continuous carbon-fiber automotive structural composites. Department of Energy; 2003.
10. Halary J-L, Lauprêtre F, Monnerie L. Polymer materials: macroscopic properties and molecular interpretations. Hoboken, N.J: Wiley; 2011.
11. The Matrix. Compos World 2015.
12. Hergenrother PM. The Use, Design, Synthesis, and Properties of High Performance/High Temperature Polymers: An Overview. High Perform Polym 2003;15(1):3–45.
13. Beyler CL, Hirschler TR. Thermal Decomposition of Polymeric Materials. SFPE Handb. Fire Prot. Eng., New York, NY: Springer New York; 2016, pp. 167–254.
14. Hinkley JA, Connell JW. Resin Systems and Chemistry: Degradation Mechanisms and Durability. In: Pochiraju KV, Tandon GP, Schoeppner GA, editors. Long-Term Durab. Polym. Matrix Compos., Boston, MA: Springer US; 2012, pp. 1–37.
15. Colin X, Verdu J. Strategy for studying thermal oxidation of organic matrix composites. Compos Sci Technol 2005;65(3-4):411–9.
16. Davies P, Rajapakse YDS, editors. Durability of Composites in a Marine Environment. Dordrecht: Springer Netherlands; 2014.
17. Weitsman YJ. Effects of Fluids on Polymeric Composites - A Review. Office of Naval Research; 1995.
18. Zhang M, Sun B, Gu B. Accelerated thermal ageing of epoxy resin and 3-D carbon fiber/epoxy braided composites. Compos Part Appl Sci Manuf 2016;85:163–71.
19. Antoon MK, Koenig JL. Irreversible effects of moisture on the epoxy matrix in glass-reinforced composites. J Polym Sci Polym Phys Ed 1981;19(2):197–212.
20. Zhou J, Lucas JP. Hygrothermal effects of epoxy resin. Part I: the nature of water in epoxy. Polymer 1999;40(20):5505–12.
21. Zhou J, Lucas JP. Hygrothermal effects of epoxy resin. Part II: variations of glass transition temperature. Polymer 1999;40(20):5513–22.
22. Technical Data Sheet: Cytec CYCOM 977-20 epoxy resin 2017.
23. EPON Resin Structural Reference Manual. Shell Chemical Company; 1989.